Chemical Reaction of Nitric Oxides with the 5-1DB Defect of the Single-Walled Carbon Nanotube

Lei Vincent Liu, Wei Quan Tian,† and Yan Alexander Wang*

Department of Chemistry, University of British Columbia, Vancouver, British Columbia V6T 1Z1, Canada

Received: July 17, 2005; In Final Form: November 21, 2005

In this work, we applied a two-layered ONIOM (B3LYP/6-31G(d):UFF) method to study the reaction of nitric oxides with a 5-1DB defect on the sidewall of the single-walled carbon nanotube (SWCNT). We have chosen a suitable ONIOM model for the calculation of the SWCNT based on the analyses of the frontier molecular orbitals, local density of states, and natural bond orbitals. Our calculations clearly indicate that the 5-1DB defect is the chemically active center of the SWCNT. In the reaction of nitric oxides with the defected SWCNT, the 5-1DB defect site can capture a nitrogen atom from nitric oxides, yielding the N-substitutionally doped SWCNT. We have explored the reaction pathway in detail. Our work verifies the chemical reactivity of the 5-1DB defects of the SWCNTs, indicates that the 5-1DB defect is a possible site for the functionalization of the SWCNTs, and demonstrates a possible way to fabricate position controllable substitutionally doped SWCNTs with a low doping concentration under mild conditions via some simple chemical reactions.

Introduction

Since the discovery of carbon nanotubes (CNTs) by Iijima,[1] thousands of scientists have joined the research field of CNTs owing to their fascinating mechanical, thermal, and electrical properties and various promising applications, including hydrogen storage,[2] chemical sensors,[3] and nanobioelectronics,[4] etc.

The B- and N-substitutionally doped CNTs have received significant attention from theoretical and experimental scientists.[5−14] Peng et al. pointed out that the B- and N-substitutionally doped CNTs can be used as sensitive and selective chemical sensors;[5] Choi et al. showed that acceptor and donor states will occur near the Fermi level after substitutional doping of B and N into the CNTs, which leads to the *p*-type and *n*-type CNTs and broadens their application in nanoelectronics;[6] Blase et al. indicated that the B- and N-substitutionally doped CNTs are possible candidates for nanosize electronic and photonic devices with various electronic properties.[7] By using the generalized tight-binding molecular dynamics method, Srivastava et al. showed that the nitrogen atom (if produced as free gas-phase neutral atoms) can be substitutionally doped into the SWCNTs, mediating the vacancy.[9]

Nowadays, there are several successful synthesis methods for the B- and N-substitutionally doped CNTs, including substitution reactions by thermal treatment,[10] chemical vapor deposition,[11] arc method,[12] and laser ablation,[13] etc. But, all these methods require critical conditions of very high temperatures of hundreds to thousands of degrees and cannot control the doping positions and concentration of heteroatoms on the sidewall of the SWNCT.[10−14] It has been recently recognized that low doping concentrations may enhance the electric conductance and leave the mechanical properties of the CNTs almost unchanged.[14] However, the reported experimental and theoretical studies on the B- and N-substitutionally doped SWNCTs are scarce.[14] It is our hope that our work will provide some theoretical guidance in this important, emerging new field.

A single vacancy that has three two-coordinated carbon atoms may be artificially introduced by ion and electron irradiation[15,16] or exist as native defects.[17] For the SWCNTs with small diameters, a single vacancy (Figure 1a) with three dangling bonds (DBs) is only metastable: two of these three two-coordinated carbon atoms will recombine to form a much more stable pentagon carbon ring, leaving the third two-coordinated carbon atom with one dangling bond and forming the so-called 5-1DB defect,[16,18] as shown in Figure 1b,c. (Throughout the entire text, the acronym 5-1DB means that the single vacancy defect site contains one five-membered carbon ring and one carbon atom with one dangling bond.) The vacancies and dangling bonds on the SWCNTs may play the role of chemical connectors of two defected nanotubes,[19] a chemisorption site for acetone[20a] and hydrogen gas,[20b] and a chemical reaction site for nitrogen dioxide.[20c] The existence of the 5-1DB defects may provide us a possible new way to functionalize the sidewall of the SWCNT.

In this paper, we will first assess the chemical reactivity of the 5-1DB defects from the analyses of the frontier molecular orbitals (FMOs) and local density of states (LDOS). Then, we will study the reaction of nitric oxides (NOs) with the 5-1DB defect on the SWCNT. We will show that it is highly possible to fabricate position-controllable N-substitutionally doped SWCNTs with low doping concentrations under mild conditions. To our knowledge, nobody has reported any theoretical studies about how to use some simple chemical reactions of the 5-1DB defects on the SWCNT to fabricate position-controllable N-substitutionally doped SWCNTs with low doping concentrations under mild conditions.

Computational Methods and ONIOM Model Selection

We first prepared a fragment of the (5,5) SWCNT ($C_{200}H_{20}$), which has 200 carbon atoms and 20 capping hydrogen atoms at the two ends. Then, we removed a carbon atom from the center of the (5,5) SWCNT segment to create a single vacancy,

* Corresponding author. E-mail: yawang@chem.ubc.ca.
† Current address: Department of Material Science, Faculty of Engineering Sciences, Kyushu University, 6-1 Kasugakoen, Kasuga, Fukuoka, 816-8580, Japan.

10.1021/jp053931b CCC: $33.50
Published on Web 01/12/2006

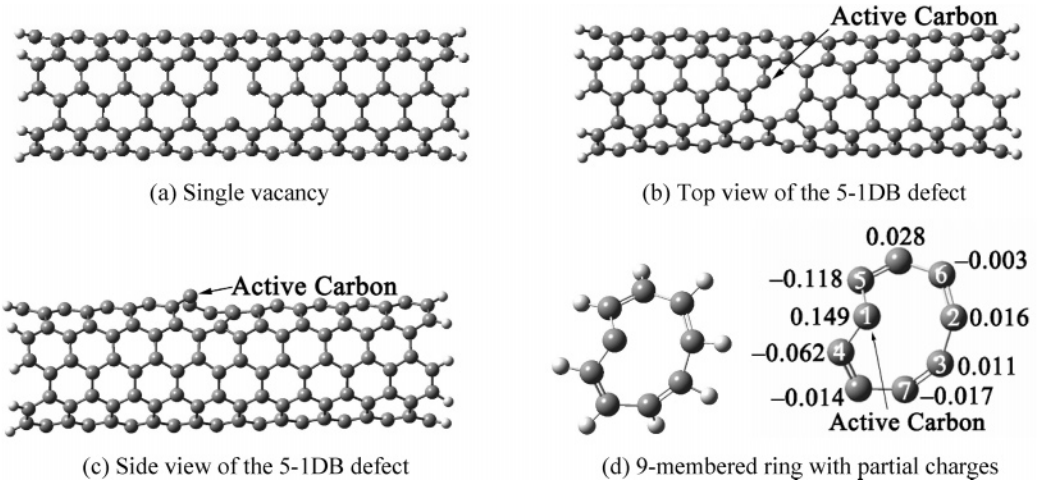

Figure 1. (a) Single vacancy on the (5,5) SWCNT. (b) Top view of the 5-1DB defect on the (5,5) SWCNT, where the nine-membered ring is chosen as the high layer and the other carbon atoms are chosen as the low layer in a two-layered ONIOM model. (c) Side view of the 5-1DB defect on the (5,5) SWCNT, where the active carbon atom sticks out of the sidewall surface of the SWCNT. (d) Nine-membered ring (with partial charges) of the 5-1DB defect capped by hydrogen atoms. The double lines in panel d denote the C═C double bonds.

as shown in Figure 1a. We initially applied the semiempirical MNDO-PM3 methond[21] to optimize the geometries of $C_{200}H_{20}$ and the SWCNT with a single vacancy ($C_{199}H_{20}$) and then fully optimized the geometries within the hybrid density functional method B3LYP[22,23] with the 6-31G basis set. We have carried out both of the spin-restricted and the spin-unrestricted DFT calculations and found that for both $C_{200}H_{20}$ and $C_{199}H_{20}$, the spin-unrestricted DFT calculations always converge to the spin-restricted DFT wave functions. This clearly indicates that the SWCNT with a single vacancy is a closed-shell singlet carbene.

For the optimized structure of the SWCNT with a single vacancy, we obtained the 5-1DB defected SWCNT as shown in Figure 1b,c. One can see that there is a carbon atom (called the active carbon atom hereafter) that stays out of the sidewall surface of the SWCNT. This out-of-surface geometry will facilitate the active carbon atom to react with incoming molecular or atomic species, due to the smaller steric hindrance when compared with other carbon atoms near the 5-1DB defect site.[20]

ONIOM, an acronym for our own N-layered integrated molecular orbital and molecular mechanics, is a method pioneered by Morokuma[24] and is widely used for the studies of SWCNTs.[25−27] In an ONIOM model, up to three layers can be treated in the calculation of a large molecular system, and different theoretical methods can be applied for different layers. In general, the dangling bonds of each layer at the boundary should be capped by atoms so that the resulting bonds at the boundary closely resemble the original chemical environment and bond characters. In this study, hydrogen atoms were used as the capping atoms. When using ONIOM, one has to choose an appropriate partition of the system into the high- and low-level layers and assign suitable methods for different layers. The most important rule is including the major players (chemically active atoms) of the system in the high-level layer and the minor players in the low-level layer.[28] To choose a suitable ONIOM model, we did the following calculations.

Single-point calculations for $C_{200}H_{20}$ and the (5,5) SWCNT with a 5-1DB defect were performed at the B3LYP/6-31G level of theory. We found that its gap between the highest occupied molecular orbital (HOMO) and the lowest unoccupied molecular orbital (LUMO) is 0.84 eV, which is smaller than the gap of $C_{200}H_{20}$ (1.38 eV). This is due to the relaxation of the geometric constraint of the SWCNT after the removal of one carbon atom,

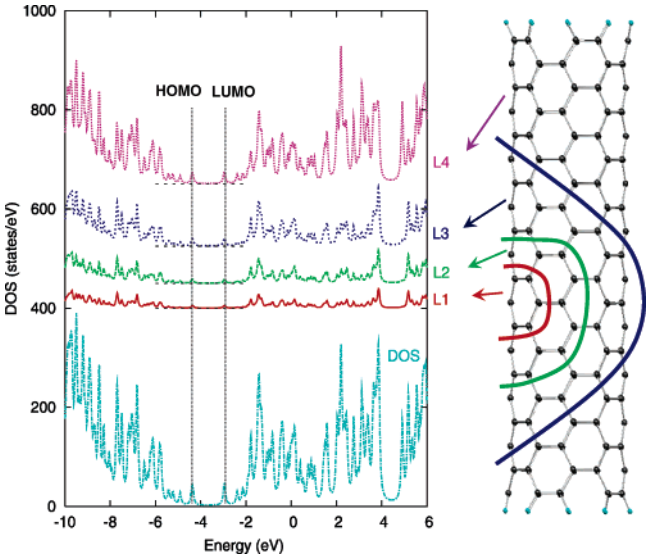

Figure 2. Total and local densities of states for the open-end (5,5) SWCNT segment $C_{200}H_{20}$ with the D_{5d} symmetry. HOMO is the highest occupied molecular orbital with orbital energy −4.35 eV, and LUMO is the lowest unoccupied molecular orbital with orbital energy −2.97 eV. L1, L2, L3, and L4 are local density of states for each specified layer of $C_{200}H_{20}$ as outlined on the structure.

which destabilizes the HOMO and stabilizes the LUMO. The LDOS of different regions in $C_{200}H_{20}$ corresponding to the (5,5) SWCNT with a 5-1DB defect are plotted in Figures 2 and 3 to illustrate how the 5-1DB defect affects the electronic structure of the (5,5) SWCNT. We found that for $C_{200}H_{20}$, the LDOS of each layer are very similar and contribute equally to the FMOs and that there is no localized electronic state on $C_{200}H_{20}$. For $C_{199}H_{20}$, we found that the contribution to the HOMO and the LUMO from the nine-membered ring (L1 in Figure 3) of the (5,5) SWCNT with a 5-1DB defect is much bigger than that of the corresponding region (L1 in Figure 2) in $C_{200}H_{20}$. The FMOs of $C_{199}H_{20}$ are shown in Figure 4. One can find that the 5-1DB defect strongly destructs the conjugated π system of $C_{200}H_{20}$. The HOMO of $C_{199}H_{20}$ mainly consists of lone-pair electrons of the active carbon atom and the π bonds of the other carbon atoms of the nine-membered ring. For the LUMO of $C_{199}H_{20}$, the nine-membered ring, especially the active carbon atom, has the dominate contribution, while only half of the sidewall of

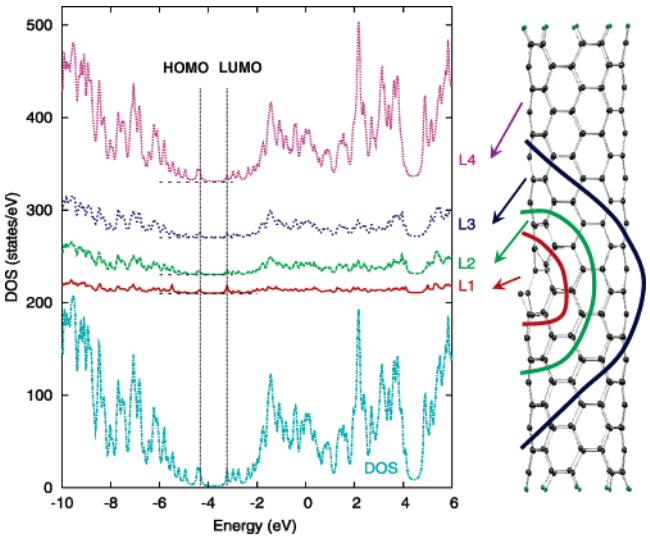

Figure 3. Total and local density of states of the open-end (5,5) SWNCT with a 5-1DB defect, $C_{199}H_{20}$. HOMO is the highest occupied molecular orbital with orbital energy −4.21 eV, and LUMO is the lowest unoccupied molecular orbital with orbital energy −3.37 eV. L1, L2, L3, and L4 are local density of states for each specified layer of $C_{199}H_{20}$ as outlined on the structure.

the SWCNT contributes to the LUMO. Clearly, the 5-1DB defect leads to the existence of localized electronic states and hosts the regioselective reactive region on the sidewall of the SWCNT. Furthermore, according to the natural bond orbital (NBO) analysis, there are four C═C double bonds in the nine-membered ring of the 5-1DB defect (see Figure 1d), and the nine-membered ring connects to its neighboring carbon atoms via C−C single bonds, which are ideally replaced by the buffering C−H single bonds in the ONIOM model. So, we treated the nine-membered ring as the major player of the 5-1DB defected SWCNT system.

To verify this assessment, we performed a single-point calculation of the nine-membered ring of the 5-1DB defect capped by hydrogen atoms (C_9H_8 shown in Figure 1d) also at the B3LYP/6-31G level of theory. After comparing the FMOs of $C_{199}H_{20}$ and C_9H_8, we found that the HOMO and LUMO of $C_{199}H_{20}$ were very close to those of C_9H_8, as shown in Figure 4. According to Fukui's frontier orbital theory,[29] the HOMO and the LOMO are the most important molecular orbitals in chemical reactions. We hence concluded that the nine-membered ring of the 5-1DB defect, especially the active carbon atom, is the chemically active center and that the C_9H_8 model can be used to represent most of the chemical properties of the 5-1DB defect on the SWCNT.

On the basis of the previous discussion, we decided to use a two-layered ONIOM model for the system. We included the nine-membered ring of the 5-1DB defect and NOs in the high layer, which was treated at the B3LYP/6-31G(d) level of theory, and all the other carbon atoms in the low layer were treated by the universal force field (UFF).[30] In fact, this is the only logical way to define the high layer of the ONIOM model because the nine-membered ring connects to its neighboring carbon atoms in the SWCNT via C−C single bonds, which are ideally replaced by the buffering C−H single bonds in the ONIOM model. To incorporate more neighboring carbon atoms around the nine-membered ring into the expanded high layer of the ONIOM model will inevitably cut many aromatic C═C double bonds, hence drastically changing the electronic structure of the SWCNT.

Although the same level different basis set (SLDB) method is highly recommended for the treatment of the SWCNTs by Kar et al.,[31] it can introduce artificial charge polarization and transfer due to the fact that electrons stay near the atoms with more basis functions. Hence, we did not use the SLDB method in our studies.

The Hessian was calculated to verify the nature of all the stationary points (transition states or local minima). The partial charges and NBOs were studied by using the NBO 3.1[32] module in the Gaussian 03 package.[33] The spin-unrestricted DFT method was applied to all open-shell species. All calculations were done using the Gaussian 03 package.[33]

To obtain the energetics, single-point calculations of all the reactants, the transition states, the intermediates, and the final product were performed at the B3LYP/6-31G level of theory for the optimized geometries obtained from the ONIOM model. We term this scheme the ONIOM/DFT scheme, in which single-point DFT calculations, based on the optimized structures within

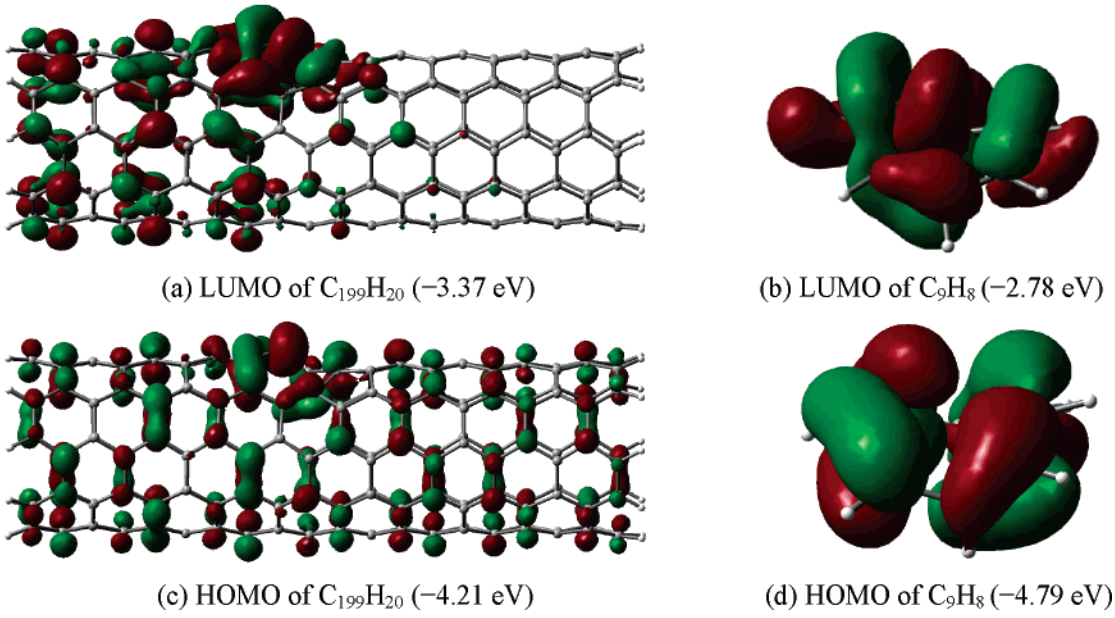

Figure 4. Frontier molecular orbitals of $C_{199}H_{20}$ and C_9H_8. The numbers in parentheses are the orbital energies in eV.

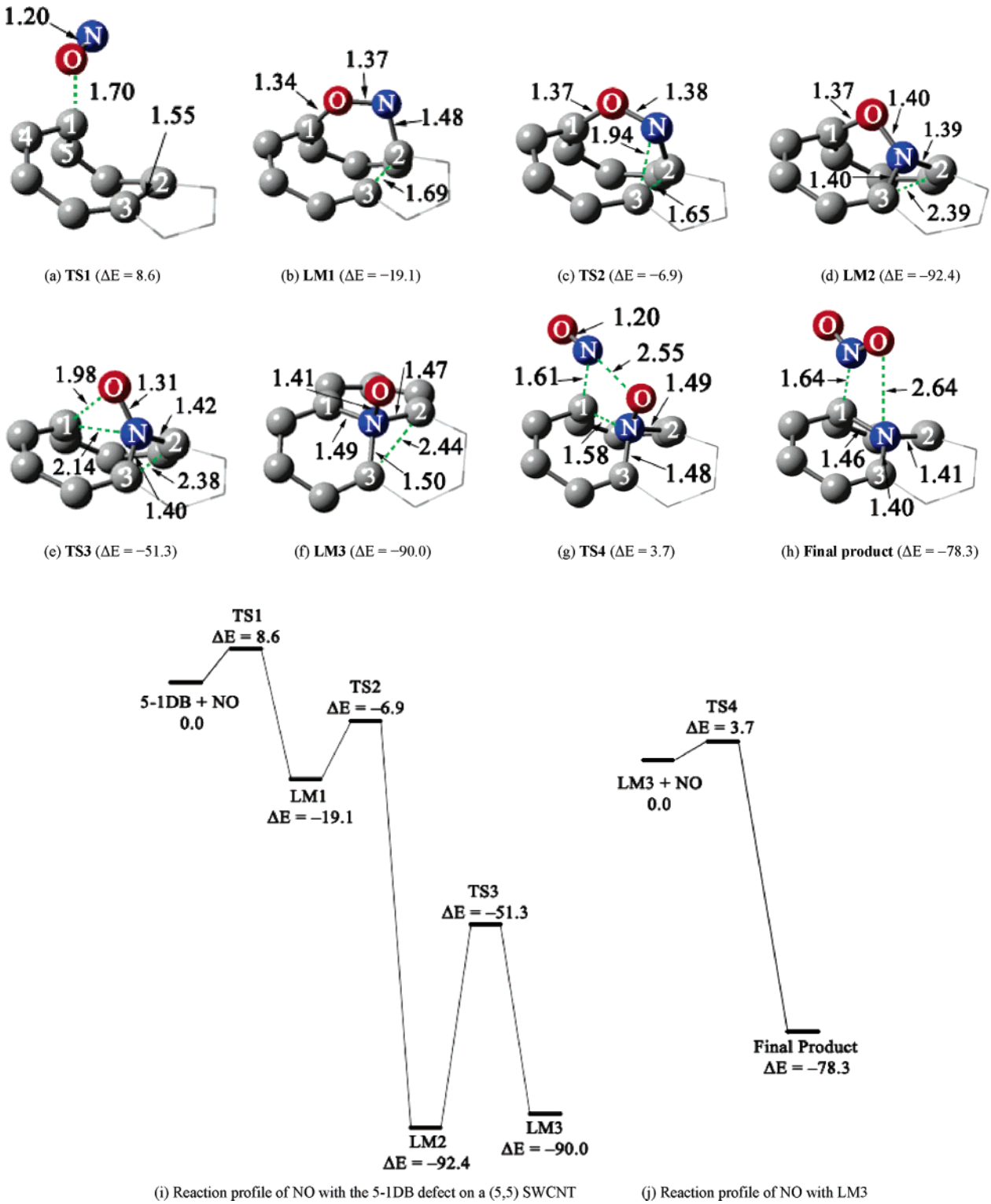

Figure 5. Reaction profiles and geometries of the transition states, the intermediates, and the final product of the reaction of NOs with $C_{199}H_{20}$. The units of energy and bond length are in kcal/mol and Å, respectively. The active carbon atom is labeled as Carbon 1, and the other two important carbon atoms are labeled as Carbons 2 and 3. The nitrogen atoms are in blue, and the oxygen atoms are in red. Only those atoms in the high layer of the ONIOM model are shown here.

the ONIOM model, are used to obtain the total energies. This ONIOM/DFT scheme has been benchmarked against fully converged DFT optimizations of several intermediate states of the system we studied here, and the data provided in the Supporting Information show that the ONIOM/DFT scheme can reproduce the structures and the energy differences of the full DFT results quite well.

Results and Discussion

Attack of the First NO. The active carbon atom C1 forms bonds with its two neighboring carbon atoms, C4 and C5, as shown in Figure 5a. On the basis of the NBO analysis, there are two two-center σ NBOs involving the active carbon atom: σ (C1−C4) = 0.678 C1 ($sp^{1.95}$) + 0.735 C4 ($sp^{2.00}$) and σ (C1−C5) = 0.676 C1 ($sp^{2.06}$) + 0.736 C5 ($sp^{2.04}$). There are two

lone-pair-type NBOs for the active carbon atom: one is an $sp^{2.01}$ hybridized orbital with 1.51 electrons, and the other one is a pure p orbital with 0.51 electrons. Hence, the active carbon atom is clearly sp^2 hybridized. The NBO partial charges for carbon atoms of the nine-membered ring are shown in Figure 1d. Only the active carbon atom and its two immediate neighbors, C4 and C5, have relatively large partial charges, and the active carbon atom has the largest partial charge, which means that the active carbon atom will have the largest electrostatic effects.

As discussed previously, the active carbon atom C1 has the smallest steric hindrance and is the most chemically reactive center. We consequently considered two initial attacking modes of NO toward C1, O-end attacking and N-end attacking, and we only found a transition state for the O-end attacking mode. This can be rationalized from the electrostatic effect. When NO is far away from C1, the orbital interaction effect is very small, and the electrostatic effect should be the dominant factor controlling the initial reaction. The NBO partial charges of NO are distributed as N(+0.181)═O(−0.181), whereas the active carbon atom has a +0.149 partial charge. This explains why we only found the O-end attacking transition state. The geometry of this transition state (**TS1**) is shown in Figure 5a. The C2−C3 bond length is 1.55 Å, a typical C−C single bond. The distance between O and C1 is 1.70 Å. The energy barrier is only 8.6 kcal/mol, which means that the initial attacking is very feasible, mainly due to the strong electrostatic attraction and molecular orbital overlap between O and C1. At this stage, the pentagon of the 5-1DB defect still exists, and there are 0.052 electrons transferred from SWCNT to NO. From the shapes and energies of the FMOs of **TS1**, NO and the SWCNT with the 5-1DB defect, the orbital interaction for **TS1** can be viewed as the singly occupied molecular orbital (SOMO) of NO interacting with the HOMO of the SWCNT with the 5-1DB defect.

After overcoming the initial reaction barrier, the system reaches the first intermediate, **LM1** (shown in Figure 5b), with a bridge configuration. The oxygen atom is still chemically bounded to C1, and the nitrogen atom begins to form a chemical bond with C2. When O approaches C1, N also approaches C2, with an in-phase orbital overlap. The energy of **LM1** is 19.1 kcal/mol lower than that of the reactants (i.e., the initial reaction is exothermic).

In **LM1**, the pentagon begins to open, the C2−C3 bond is slightly broken with an elongated bond length 1.69 Å (quite close to 1.55 Å in **TS1**), and the double bond characters of C2═C6 and C3═C7 are still preserved (see Figure 1d). Clearly, even when the C2−C3 bond is partially broken, C2 and C3 still connect to their neighboring carbon atoms in the low layer via C−C single bonds. This fact offers strong support for our partitioning scheme of the two-layered ONIOM model. With the partial breaking of the C2−C3 bond, C3 in **LM1** becomes a new active center because it has one potential dangling bond upon a complete breaking of the C2−C3 bond.

The geometry of **TS2** is shown in Figure 5c. The distance between N and C3 is 1.94 Å, indicating the bond forming and breaking motions at **TS2**. The system can easily overcome this energy barrier of 12.2 kcal/mol from **LM1** to **TS2**, which is smaller than the energy released from the initial reaction (19.1 kcal/mol). After crossing **TS2**, the system reaches **LM2** (shown in Figure 5d). In **LM2**, C2 and C3 separate further away with a distance of 2.39 Å. N forms bonds with C2 and C3 with bond lengths of 1.39 and 1.40 Å, respectively, resulting in a six-membered ring of five carbon atoms and one nitrogen atom. The formation of **LM2** is highly exothermic: the system releases 85.5 kcal/mol. Such a large amount of energy release will assist the system to move further and even break some strong bonds.

The geometries of **TS3** and **LM3** are shown in Figure 5e,f. In **TS3**, the nitrogen atom attacks C1 and the oxygen atom breaks away from C1, which is a pseudo-S_N2 reaction. The structure of **TS3** clearly indicates that it connects to the two intermediates that have either O or N bonded to C1. Although the energy barrier for **TS3** is as high as 41.1 kcal/mol, the previous steps already have released enough energy to help the system overcome this barrier. For **LM3**, one can see that N forms single bonds with C1, C2, and C3 and also with O. The oxygen atom sticks out of the sidewall of the nanotube. The energy of **LM3** is 90.0 kcal/mol lower than that of the reactants, and it is only 2.4 kcal/mol higher than **LM2**, indicating that **LM3** is quite stable. In conclusion, the net reaction of NO with $C_{199}H_{20}$ is that NO inserts its N into the defect site with the initial attack of O toward the active carbon atom. This reaction is highly thermally feasible (Figure 5i).

Attack of the Second NO. On the basis of the NBO analysis, there are three two-center NBOs involving N and its three neighboring carbon atoms in **LM3**: σ(N−C1) = 0.800 N($sp^{2.78}$) + 0.600 C1($sp^{3.05}$), σ(N−C2) = 0.801 N($sp^{2.72}$) + 0.599 C2-($sp^{2.91}$), and σ(N−C3) = 0.800 N($sp^{2.78}$) + 0.600 C3($sp^{2.95}$). It is obvious that the NBOs of these three carbon atoms have high p character. N also forms a σ bond with O, σ(N−O) = 0.751 N($sp^{3.99}$) + 0.660 O($sp^{7.41}$), with a bond length of 1.41 Å. The NBO orbital coefficients of N and O in σ(N−O) clearly indicate that it is mainly the head-to-head overlap of sp^3 hybridized orbitals of N and one p orbital of O. The unpaired electron is mostly localized on O, which has a −0.574 partial charge. The relatively long bond distance between N and O (1.41 Å) indicates that O is not strongly bounded to N, so this N−O bond may be easily broken upon proper attack from another NO molecule in the NO excess environment. Therefore, we considered the attack of a second NO toward **LM3** ($C_{199}H_{20}$-NO).

The transition state **TS4** is shown in Figure 5g. In **TS4**, the N end of the second NO attacks C1 and O1 (the oxygen atom of the first NO). The distance between C1 and N2 (the nitrogen atom of the second NO) is 1.61 Å; the C1−N1 (the nitrogen atom of the first NO) bond elongates to 1.58 Å; and the distance between N2 and O1 is 2.55 Å. The electrostatic attraction between N2 and O1 stabilizes **TS4**, whereas the electrostatic repulsion between C1 and N2 counterbalances this attraction. The overall interaction of these two reactants renders the reaction barrier for **TS4** to be only 3.7 kcal/mol: this reaction is very facile.

Following the vibrational mode of the imaginary frequency, we found the final product, a complex of NO_2 with $C_{199}NH_{20}$, which is shown in Figure 5h. In the final product, NO_2 bonds to $C_{199}NH_{20}$ through a long ionic N2−C1 bond with a bond length of 1.64 Å, and the interaction between the oxygen atom (O1) of NO_2 and the nitrogen atom (N1) of $C_{199}NH_{20}$ is very weak with a bond distance of 2.64 Å. In an experiment setting, NO_2 can be removed from the surface of the SWCNT by a flow of Ar gas.[3] The formation of the final product releases 78.3 kcal/mol energy from the reaction of the second NO with $C_{199}H_{20}NO$. The forward reaction barrier is only 3.7 kcal/mol, but the reverse reaction barrier is as high as 82.0 kcal/mol, which means that the reverse reaction is kinetically virtually impossible under normal conditions.

In summary, the second NO extracts the oxygen atom from $C_{199}H_{20}NO$, forming NO_2 and the N-substitutionally doped SWCNT through a one-step reaction (Figure 5j). This reaction

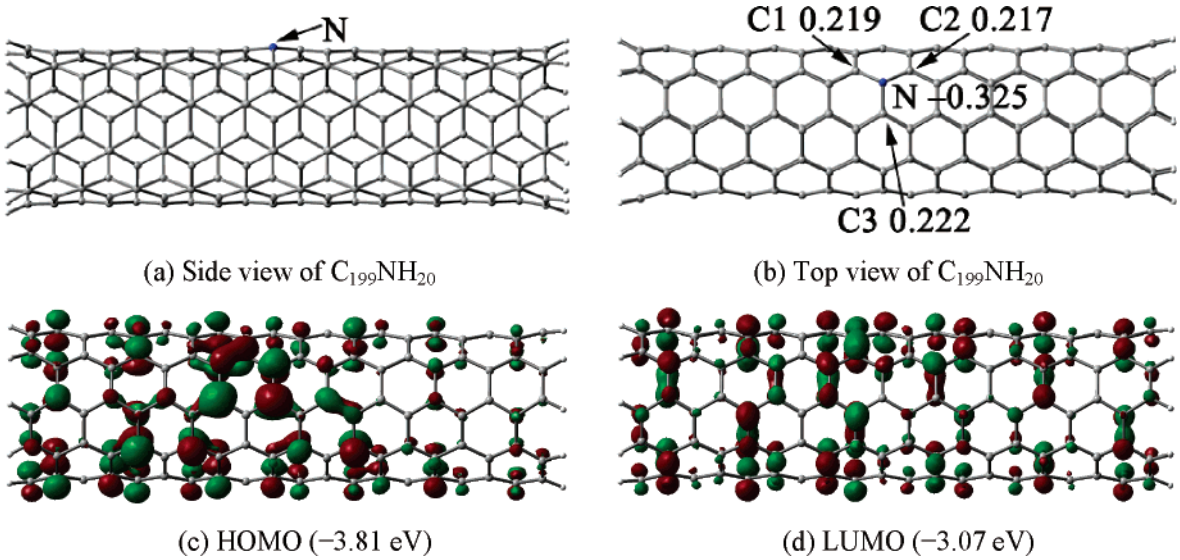

Figure 6. Structure, partial charges, and FMOs of the N-substitutionally doped (5,5) SWCNT. The numbers in parentheses are the orbital energies in eV.

can be explained by the FMO analysis. When N2 attacks C1, the positive lobe of the SOMO on N2 of the second NO has an in-phase overlap with the HOMO on C1 of **LM3**. At the same time, the negative lobe of the SOMO on N2 also has an in-phase overlap with the HOMO on O of **LM3**. These effective molecular orbital overlaps make the one-step reaction possible.

Structure optimization and NBO analysis were also performed for the N-substitutionally doped (5,5) SWCNT ($C_{199}NH_{20}$). The doped N stays a little bit above the sidewall surface of the SWCNT (Figure 6a) because of the longer σ(C−N) bonds and the asymmetric sp^3 hybridization of N. The partial charges are shown in Figure 6b. The band gap is only 0.74 eV, which is smaller than those of $C_{200}H_{20}$ and $C_{199}H_{20}$ (1.38 and 0.84 eV, respectively). This means that the substitutional doping of N will decrease the band gap of the (5,5) SWCNT (i.e., increasing its conductivity). Substitutional doping of N can also destruct the conjugated π system of $C_{200}H_{20}$ and introduce localized electronic states (Figure 6c,d) similar to what the 5-1DB defect does to the pure SWCNT but to a lesser degree.

Conclusions

In conclusion, we have performed theoretical studies of the chemical reactivity of the 5-1DB defect on SWCNT by a two-layered ONIOM model. The LDOS, FMO, and NBO analyses indicate that our ONIOM model successfully captures the essence of the chemical reactivity of the system. This work clearly indicates that the 5-1DB defect on the SWCNT is chemically reactive. Thus, it can be used as the active site for the functionalization of SWCNT. We have presented a possible way to fabricate the N-substitutionally doped (5,5) SWCNT mediating the 5-1DB defect.

A rational reaction pathway has been explored in detail (Figure 5i,j). First, an NO attacks the active carbon atom of the 5-1DB defect, yielding $C_{199}H_{20}NO$, which has the nitrogen atom inserted into the sidewall of the SWCNT and the oxygen atom sticking out of the surface. Second, another NO attacks $C_{199}H_{20}$-NO, forming the final product, which has the nitrogen atom completely healing the defect site. These reactions are thermally self-catalyzed, which reveals the possibility of fabricating the heteroatom-substitutionally doped SWCNT under mild conditions. We believe that our theoretical investigation shall provide guidance for experimentalists in their future work in this area.

Acknowledgment. The financial support from the Natural Sciences and Engineering Research Council (NSERC) of Canada is gratefully acknowledged. WestGrid and C-HORSE have provided us the necessary computational resources. L.V.L. acknowledges the support from the Gladys Estella Laird Fellowship and the Charles A. McDowell Fellowship of the Department of Chemistry at the University of British Columbia. W.Q.T. received a postdoctoral fellowship from the Japan Society for the Promotion of Science (JSPS) and thanks Prof. Yuriko Aoki at Kyushu University for her hospitality.

Supporting Information Available: Some related frontier molecular orbitals of $C_{199}H_{20}$, $C_{200}H_{20}$, NO, **TS1**, **LM3**, and the N-substitutionally doped (5,5) SWCNT; energies of **LM1**, **LM2**, and **LM3** from the full DFT scheme, the ONIOM/DFT scheme, and the ONIOM scheme; and the optimized geometries of the intermediates and the transition states. This material is free of charge via the Internet at http://www.pubs.acs.org.

References and Notes

(1) (a) Iijima, S. *Nature* **1991**, *354*, 56. (b) Iijima, S.; Ichihashi, T. *Nature* **1993**, *363*, 603.

(2) Liu, C.; Fan, Y. Y.; Liu, M.; Cong, H. T.; Cheng, H. M.; Dresselhaus, M. S. *Science* **1999**, *286*, 1127.

(3) Kong, J.; Franklin, N. R.; Zhou, C. W.; Chapline, M. G.; Peng, S.; Cho, K. J.; Dai, H. J. *Science* **2000**, *287*, 622.

(4) Katz, E.; Willner, I. *ChemPhysChem* **2004**, *5*, 1085.

(5) Peng, S.; Cho, K. J. *Nano Lett.* **2003**, *3*, 513.

(6) Choi, H. J.; Ihm, J.; Louie, S. G.; Cohen, M. L. *Phys. Rev. Lett.* **1999**, *307*, 158.

(7) Blase, X.; Charlier, J.-C.; De Vita, A.; Car, R. *Appl. Phys. Lett.* **1997**, *70*, 197.

(8) Nikulkina, A. V.; D'yachkov, P. N. *Russ. J. Inorg. Chem.* **2004**, *49*, 430.

(9) Srivastava, D.; Menon, M.; Daraio, C.; Jin, S.; Sadanadan, B.; Rao, A. M. *Phys. Rev. B* **2004**, *69*, 153414.

(10) (a) Golberg, D.; Bando, Y.; Han, W.; Kurashima, K.; Sato, T. *Chem. Phys. Lett.* **1999**, *308*, 337. (b) Golberg, D.; Bando, Y.; Bourgeois, L.; Kurashima, K.; Sato, T. *Carbon* **2000**, *38*, 2017.

(11) Sung, S. L.; Tsai, S. H.; Tseng, C. H.; Chiang, F. K.; Liu, X. W.; Shih, H. C. *Appl. Phys. Lett.* **1999**, *74*, 197.

(12) (a) Stephan, O.; Ajayan, P. M.; Colliex, C.; Redlich, Ph.; Lambert, J. M.; Bernier, P.; Lefin, P. *Science* **1994**, *266*, 1683. (b) Glerup, M.; Steinmetz, J.; Samaille, D.; Stephan, O.; Enouz, S.; Loiseau, A.; Roth, S.; Bernier, P. *Chem. Phys. Lett.* **2004**, *387*, 193.

(13) (a) Zhang, Y.; Gu, H.; Suenaga, K.; Iijima, S. *Chem. Phys. Lett.* **1997**, *279*, 264. (b) Gai, P. L.; Stephan, O.; McGuire, K.; Rao, A. M.; Dresselhaus, M. S.; Dresselhaus, G.; Colliex, C. *J. Mater. Chem.* **2004**, *14*, 669.

(14) Terrones, M.; Jorio, A.; Endo, M.; Rao, A. M.; Kim, Y. A.; Hayashi, T.; Terrones, H.; Charlier, J.-C.; Dresselhaus, G.; Dresselhaus, M. S. *Mater. Today* **2004**, *7*, 30.

(15) Krasheninnikov, A. V.; Nordlund, K. *J. Vac. Sci. Technol. B* **2002**, *20*, 728.

(16) Ajayan, P. M.; Ravikumar, V.; Charlier, J.-C. *Phys. Rev. Lett.* **1998**, *81*, 1437.

(17) Charlier, J.-C. *Acc. Chem. Res.* **2002**, *35*, 1063.

(18) Krasheninnikov, A. V.; Nordlund, K.; Sirvio, M.; Salonen, E.; Keinonen, J. *Phys. Rev. B* **2001**, *63*, 245405.

(19) Terrones, M.; Terrones, H.; Banhart, F.; Charlier, J.-C.; Ajayan, P. M. *Science* **2000**, *288*, 1226.

(20) (a) Chakrapani, N.; Zhang, Y. M.; Nayak, S. K.; Moore, J. A.; Carroll, D. L.; Choi, Y. Y.; Ajayan, P. M. *J. Phys. Chem. B* **2003**, *107*, 9308. (b) Lu, A. J.; Pan, B. C. *Phys. Rev. B* **2005**, *71*, 165416. (c) Mercuri, F.; Sgamellotti, A.; Valentini, L.; Armentano, I.; Kenny, J. M. *J. Phys. Chem. B* **2005**, *109*, 13175.

(21) Stewart, J. J. P. *J. Comput. Chem.* **1989**, *10*, 209.

(22) Becke, A. D. *J. Chem. Phys.* **1993**, *98*, 5648.

(23) Lee, C. T.; Yang, W.; Parr, R. G. *Phys. Rev. A* **1988**, *37*, 785.

(24) Maseras, F.; Morokuma, K. *J. Comput. Chem.* **1995**, *16*, 1170.

(25) Walch, S. P. *Chem. Phys. Lett.* **2003**, *374*, 501.

(26) Ricca, A.; Bauschlicher, C. W.; Maiti, A. *Phys. Rev. B* **2003**, *68*, 035433.

(27) Lu, X.; Tian, F.; Xu, X.; Wang, N.; Zhang, Q. *J. Am. Chem. Soc.* **2003**, *125*, 10459.

(28) Morokuma, K. *Bull. Korean Chem. Soc.* **2003**, *24*, 797.

(29) Fukui, K. *Science* **1987**, *218*, 747.

(30) Rappe, A. K.; Casewit, C. J.; Colwell, K. S.; Goddard, W. A., III; Skiff, W. M. *J. Am. Chem. Soc.* **2004**, *114*, 10024.

(31) Kar, T.; Akdimb, B.; Duan, X.; Pachter, R. *Chem. Phys. Lett.* **2004**, *392*, 176.

(32) (a) Glendening, E. D.; Carpenter, A. E.; Weinhold, F. *NBO Version 3.1*; 1995. (b) Reed, A. E.; Curtiss, L. A.; Weinhold, F. *Chem. Rev.* **1988**, *88*, 899.

(33) Frisch, M. J. et al.; *Gaussian 03*, revision B.05; Gaussian, Inc.: Pittsburgh, PA, 2003.